

Two-phase convex-type corner flows

By J. VAL. HEALY

Aerodynamische Versuchsanstalt Göttingen, Germany

(Received 22 May 1969 and in revised form 23 December 1969)

The flow of an inviscid incompressible fluid, with imbedded identical spherical particles, around an arbitrary corner is treated by the method of small perturbations. Application is made to convex flows only and the approximate effects of separation are also considered. The assumption of arbitrary initial particle density k_0 leads to a complex system of equations, which appears to have no simple solution in general, and is not considered. For small k_0 the particle density distribution is governed by a first-order partial differential equation which, when solved by the method of characteristics, yields ordinary differential equations, whose solutions are simple and analytic for unseparated flow and numerical only when separation is considered. In the former flow, spiral type curves partially encircling the plate tip, and then trailing downstream, delineate the particle-free zones, and it is found that the particle density increases monotonically in the downstream direction on all particle streamlines. In the separated flow, the most noteworthy effect is the disappearance of the infinite velocity at the origin and the consequent considerable reduction in the magnitude of the perturbation.

1. Introduction

The flows involved in the present problem comprise an incompressible fluid, inviscid apart from the fluid-particle interaction, imbedded with small identical spherical particles. The analysis is carried out for a general corner and hence includes the flow in a wedge-shaped channel, stagnation point flow, flow around convex corners and the flow around a semi-infinite flat plate. In view of this large number of geometries, the attention here is devoted to convex type flows only, in which the separation is the most important phenomenon. To be more specific, the cases of a small convex corner angle and the flow around a semi-infinite flat plate are treated in some detail. Viscous effects are not considered, since even the corresponding problem for a single-phase fluid is not well understood. Concave type flows, in which the viscous effects are predominant, are left for a later study.

Perturbation methods are not new in the mechanics of two-phase flows. To the author's knowledge, the first application was by Rannie (1962, pp. 117–144) to the flow through nozzles. Michael (1968) used the method to study the flow past a sphere, and the present paper continues this line of investigation.

Basically, the methodology consists of perturbing an initially steady-state flow, in which the particles are so small that they follow the fluid streamlines with negligible deviation. This initial state is well known from potential flow

theory. The particles are then allowed to acquire a finite relaxation time τ , thereby perturbing the flow. Thus, equations, which are valid for small values of τ , are found.

2. The assumptions and equations

The assumptions are (1) incompressible, potential, high-speed flow, (2) fluid-particle interaction is according to Stokes' drag law, (3) the particle-particle interaction is negligible, and (4) the density of the fluid is considerably less than that of the particle material.

Subject to these assumptions, the system of equations in cylindrical coordinates is

$$u_r \frac{\partial u_r}{\partial r} + \frac{u_\varphi}{r} \frac{\partial u_r}{\partial \varphi} - \frac{u_\varphi^2}{r} = -\frac{1}{\rho} \frac{\partial p}{\partial r} - \left(\frac{u_r - v_r}{\tau} \right) k, \quad (1)$$

$$u_r \frac{\partial u_\varphi}{\partial r} + \frac{u_\varphi}{r} \frac{\partial u_\varphi}{\partial \varphi} + \frac{u_r u_\varphi}{r} = -\frac{1}{\rho r} \frac{\partial p}{\partial \varphi} - \left(\frac{u_\varphi - v_\varphi}{\tau} \right) k, \quad (2)$$

$$v_r \frac{\partial v_r}{\partial r} + \frac{v_\varphi}{r} \frac{\partial v_r}{\partial \varphi} - \frac{v_\varphi^2}{r} = \frac{u_r - v_r}{\tau}, \quad (3)$$

$$v_r \frac{\partial v_\varphi}{\partial r} + \frac{v_\varphi}{r} \frac{\partial v_\varphi}{\partial \varphi} + \frac{v_r v_\varphi}{r} = \frac{u_\varphi - v_\varphi}{\tau}, \quad (4)$$

$$\frac{\partial(r u_r)}{\partial r} + \frac{\partial u_\varphi}{\partial \varphi} = 0, \quad (5)$$

$$\frac{\partial(r k v_r)}{\partial r} + \frac{\partial(k v_\varphi)}{\partial \varphi} = 0, \quad (6)$$

where \mathbf{u} and \mathbf{v} are the velocities of the fluid and particle, respectively, p is the pressure, τ is the particle relaxation time, ρ is the fluid density, and k is the ratio of the particle to the fluid mass densities.

The perturbation yields: $\mathbf{u} = \mathbf{u}_0 + \mathbf{u}'$ and $\mathbf{v} = \mathbf{u}_0 + \mathbf{v}'$, where: \mathbf{u}'/\mathbf{u}_0 and $\mathbf{v}'/\mathbf{u}_0 \ll 1$; \mathbf{u}_0 is the equilibrium fluid-particle velocity, about which the perturbation is made, and p now assumes $p_0 + p'$. The case of arbitrary initial particle density k_0 is not difficult to analyze, but the resulting equations seem to admit only wholly numerical solutions. By assuming small k_0 , the equations can be solved analytically if no separation exists. A simple separation model yields ordinary differential equations which may be solved by numerical procedures.

Following Michael, the equations for small k_0 are

$$\mathbf{u}' = 0 = p', \quad (7)$$

$$\mathbf{v}' = -\tau(\mathbf{u}_0 \cdot \nabla) \mathbf{u}_0, \quad (8)$$

$$(\mathbf{u}_0 + \mathbf{v}') \cdot \nabla k = -k \nabla \cdot \mathbf{v}'. \quad (9)$$

3. The flow without separation

From most texts on hydrodynamics, e.g. Milne-Thomson (1968, ch. 6), the velocity potential for the unperturbed flow in a corner is

$$\phi = (\alpha/n) r^n \cos n\varphi,$$

where r and φ are the co-ordinates, $n = \pi/\beta$, β is the angle between the walls, and α is a large constant. The values of n and β for various geometries are shown in figure 1.

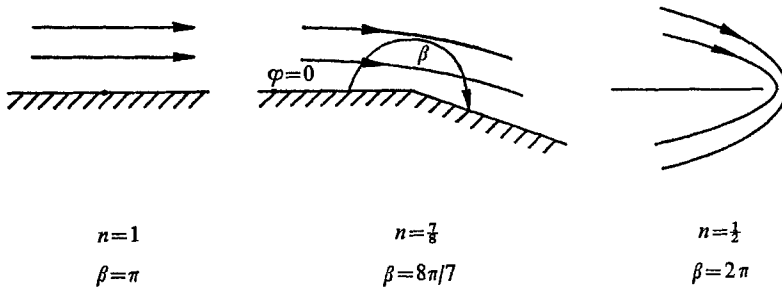


FIGURE 1. Flow configurations.

The unperturbed fluid-particle velocity components are then

$$u_{r_0} = -\alpha r^{n-1} \cos n\varphi, \quad u_{\varphi_0} = \alpha r^{n-1} \sin n\varphi. \tag{10}$$

Substituting these quantities into (8), one finds

$$\mathbf{v}' = -\tau \nabla \left(\frac{1}{2} |\mathbf{u}_0|^2 \right) = \alpha^2 \tau (n-1) r^{2n-3} \mathbf{a}, \tag{11}$$

where \mathbf{a} is a unit vector in the r direction.

Thus, to the first order, the perturbed particle velocity is independent of angle and is a simple function of r only. For values of n greater than $\frac{3}{2}$, the perturbation increases with increasing radius, while for values less than $\frac{3}{2}$, it increases with decreasing radius. The fact that, in the latter case, the perturbation becomes infinite at the origin does not render the theory invalid since, due to the extremely large fluid velocities there, no particles can approach this point. Also interesting is that the perturbation in the particle velocity is a constant, when $n = \frac{3}{2}$, i.e. when the wall angle β is 120° .

Applying the divergence operator to (11) and then combining the result with (9) and (11), one finds the equation governing the particle density

$$-(\cos n\varphi + \xi(n-1)r^{n-2}) \frac{\partial k}{\partial r} + \frac{\sin n\varphi}{r} \frac{\partial k}{\partial \varphi} = 2\xi(n-1)^2 r^{n-3} k, \tag{12}$$

where $\xi = \alpha\tau$.

Equation (12) may be solved by the method of characteristics (cf. Ince 1956, p. 47). The associated ordinary differential equations are

$$-\frac{dr}{\cos n\varphi + \xi(n-1)r^{n-2}} = \frac{r d\varphi}{\sin n\varphi} = \frac{dk}{2\xi(n-1)^2 r^{n-3} k}. \tag{13}$$

Equating the first two terms of (13) gives

$$\frac{dr}{d\varphi} + r \cot n\varphi = -\xi \frac{(n-1)r^{n-1}}{\sin n\varphi}. \tag{14}$$

Equation (14) can be recognized as a Bernoulli type (cf. Ince 1956, p. 22) and, with the transformation $r = x^{1/(2-n)}$, it becomes

$$\frac{dx}{d\varphi} + (2-n)x \cot n\varphi = \xi \frac{(n-2)(n-1)}{\sin n\varphi} \quad (n \neq 2).$$

The integrating factor for this equation is

$$\exp\left((2-n)\int \cot n\varphi d\varphi\right) = |\sin n\varphi|^{(2-n)/n},$$

and consequently one obtains

$$r^{2-n} \sin^{(2-n)/n} n\varphi - (n-2)(n-1)\xi \int \sin^{2(1/n)-1} n\varphi d\varphi = c, \tag{15}$$

for the first characteristic surfaces. A study of (10) and (11) shows that (14) also defines the particle streamlines and, therefore, the latter form the characteristic base curves. In the limit $\xi \rightarrow 0$, (15) reduces to the form $r^n \sin n\varphi = c$, which is the equation of the unperturbed streamlines.

Since n may be a fraction or an integer, no standard integral is available for (15), but for certain values of n the integration is easily carried out. For example, when $n = \frac{1}{2}$, one has

$$\left(r^{\frac{1}{2}} \sin \frac{1}{2}\varphi\right)^3 - \frac{3}{8}\xi(\varphi - \sin \varphi) = c. \tag{16}$$

Returning to (13); equating the second and third terms shows

$$\frac{dk}{d\varphi} = \frac{2\xi(n-1)^2 kr^{n-2}}{\sin n\varphi}.$$

Then, substituting for r from (15) and rearranging, one finds the relation, which is valid along a streamline c ,

$$\frac{dk}{k} = 2\left(\frac{n-1}{n-2}\right)\frac{df}{f},$$

where $f = c + (n-2)(n-1)\xi \int \sin^{2(1/n)-1} n\varphi d\varphi.$

The integral surface of (12) is then given by

$$\frac{k}{k_0} = \left[1 + (n-2)(n-1)\frac{\xi}{c} \int \sin^{2(1/n)-1} n\varphi d\varphi\right]^{2(n-1)/(n-2)}, \tag{17}$$

where the arbitrary function has been chosen such that $k = k_0 = \text{constant}$, when $\xi \rightarrow 0$.

When $n = \frac{1}{2}$, (17) reduces to

$$\frac{k}{k_0} = \left(1 + \frac{3\xi}{8c}(\varphi - \sin \varphi)\right)^{\frac{3}{2}}. \tag{18}$$

These equations indicate that k always increases along the particle streamlines and this would seem to violate particle conservation. The explanation lies in a closer examination of (15) or (16), the particle streamline equations.

The innermost particle streamline for $n = \frac{1}{2}$, found by setting $c = 0$ in (16), is given by

$$r = \left[\frac{3}{8}\xi(\varphi - \sin \varphi)\right]^{\frac{2}{3}}/\sin^2 \frac{1}{2}\varphi, \tag{19}$$

which is the equation of a spiral centred at the origin and trailing downstream. This spiral, as shown in figure 2, delineates the single and two phase zones in the fluid, and becomes asymptotic to the fluid streamline

$$r^{\frac{1}{2}} \sin \frac{1}{2}\varphi = c = \left(\frac{3}{4}\pi\xi\right)^{\frac{1}{2}}$$

far downstream and becomes more tightly wrapped for smaller particles, coinciding with the plate in the limit $\xi \rightarrow 0$. The lack of particles between the spiral and the plate accounts for the result of (17) and (18) which shows that k increases only.

The maximum value of k in the flow occurs far downstream on this spiral, i.e.

$$\frac{k_{\max}}{k_0} = \frac{k}{k_0} \Big|_{\substack{c = (\frac{3}{4}\pi\xi)^{\frac{2}{3}} \\ \varphi \rightarrow 2\pi}} = [1 + (\frac{3}{4}\pi\xi)^{\frac{2}{3}}]^{\frac{3}{2}}$$

When $\xi = 0.1$, this ratio is roughly 1.23. It should be mentioned, however, that these values of k are of limited use, since the derivatives in (12) are undefined on the delineation lines.

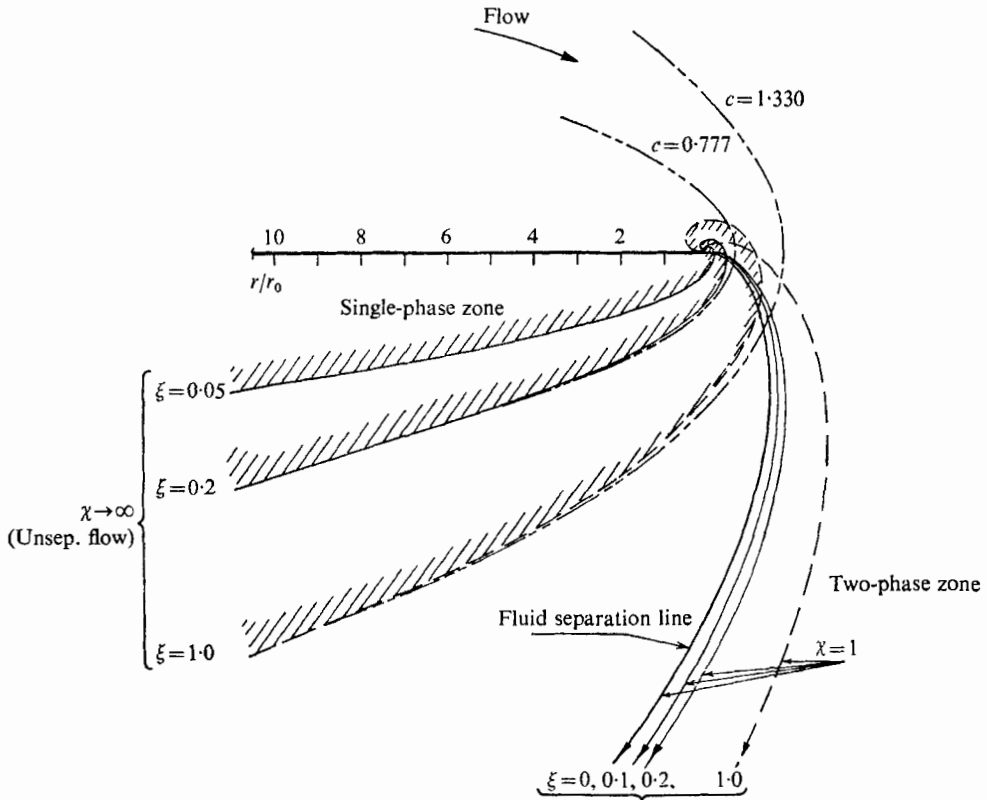


FIGURE 2. Zone delineation curves, $n = \frac{1}{2}$. - - -, fluid streamlines, $c = (\frac{3}{4}\pi\xi)^{\frac{2}{3}}$.

The curves presented for $n = \frac{7}{8}$ have been calculated from the equations of this section. For $n = \frac{1}{2}$, it is found easier to use the results of the next section on separation effects, by allowing the source strength to vanish. In this manner, a comparison between separated and unseparated flows is obtained.

The delineation curves for $n = \frac{7}{8}$ have been found by using Simpson's rule and (15), and are plotted in figure 3. The spirals are qualitatively the same as those for $n = \frac{1}{2}$, but are much less separated now and, therefore, the particle-free zones much smaller. The particle streamlines further out from the corner show

a progressively smaller deviation with ξ , from the unperturbed streamlines. Also noticeable is the much diminished size of the perturbation in general, by comparison with the unseparated case of $n = \frac{1}{2}$, as shown in figure 4.

The particle density distribution along the (particle) streamlines of figure 3 is computed from (17), for $n = \frac{7}{8}$, and plotted in figure 5. The previous observa-

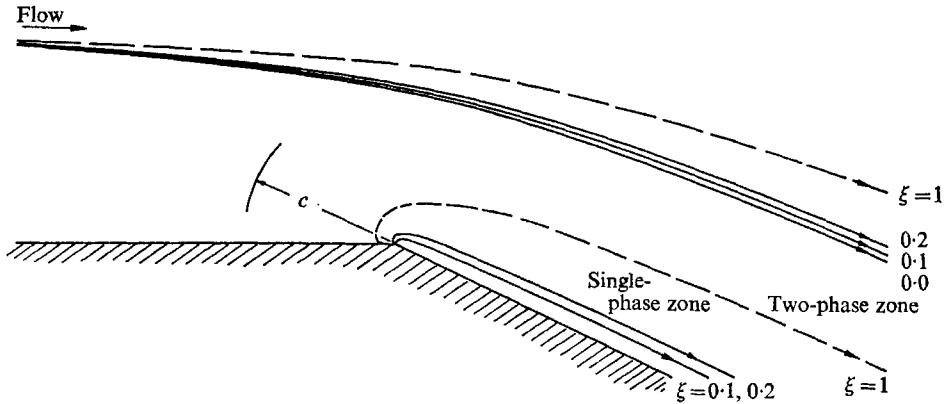


FIGURE 3. Zone delineation curves and particle streamlines, $n = \frac{7}{8}$.

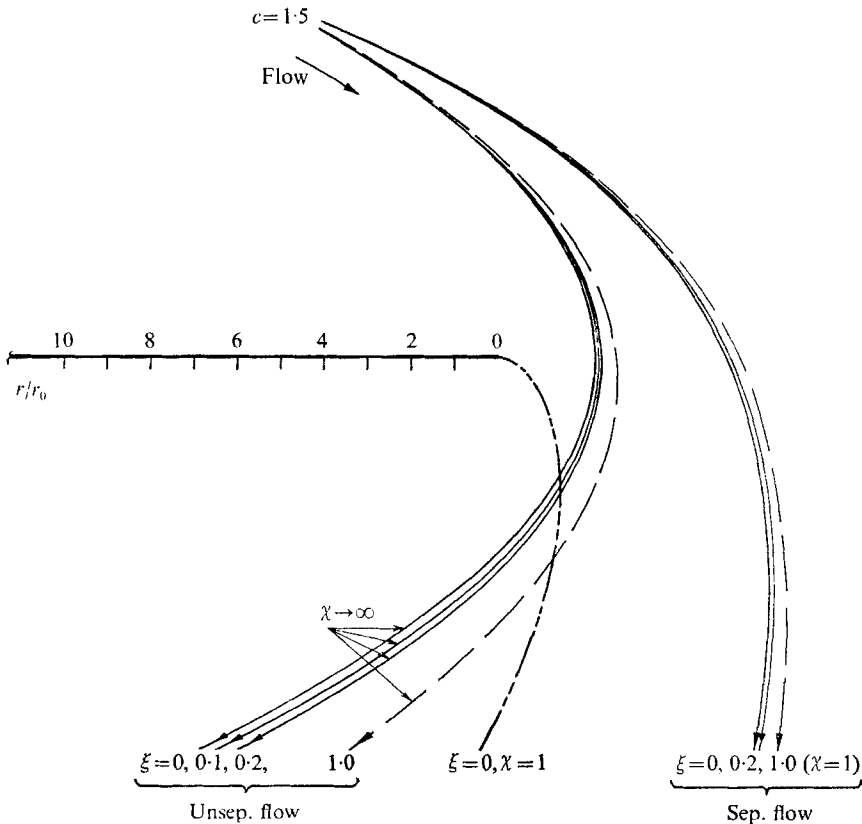


FIGURE 4. Particle streamlines, $n = \frac{1}{2}$. - - - -, fluid separation line.

tions regarding the monotonic increase in the downstream direction and the rapid diminution of the perturbation with distance from the corner are verified by these curves.

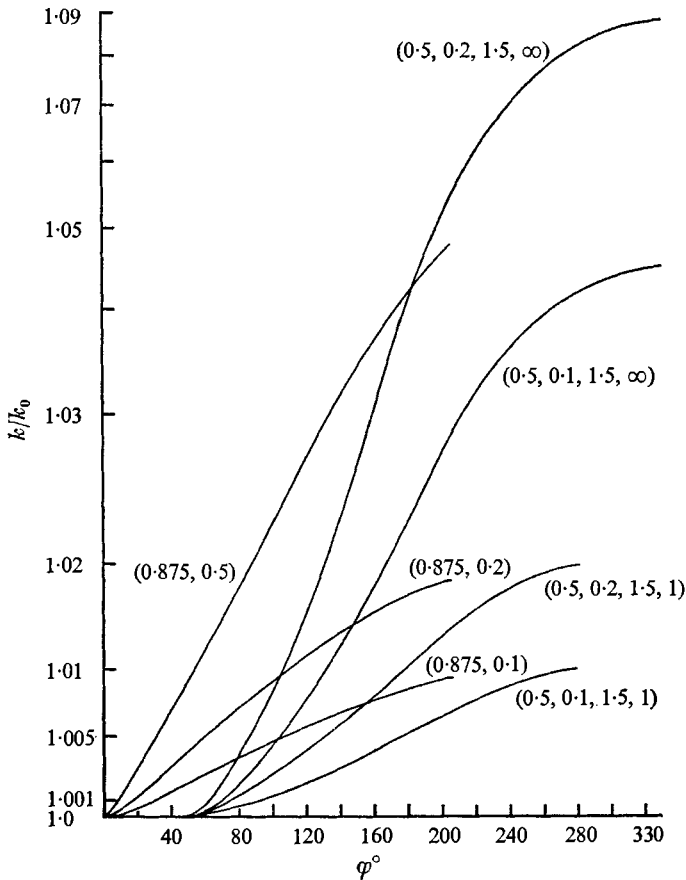


FIGURE 5. Particle density distributions. Curves: (n, ξ, c, χ) , $(n, \xi/c)$.

4. The flow with separation

Two approaches to the problem of separation seem possible; the first being the use of the free-streamline theory, and the second, that of combining the flow from a source in the wall downstream of the corner with the unseparated corner flow used previously. Although the former would probably give a more realistic picture, the theory does not lead to functions that are simple enough to be treated in the manner required in the present work. The unperturbed separated flow at the corner may be obtained in a tabular form by using the Kirchoff method, but considerably more numerical work is required to find the particle solutions. For this reason the second method is chosen.

The addition of the source complicates the corner flow so much that a simple wholly analytical solution, as presented in §3, does not exist. The algebraic work, however, can be considerably reduced by the use of the conjugate co-ordinate

system. The particle density equation is derived in this system, solved by the method of characteristics, and the Runge–Kutta process used to find the particle streamlines and density distributions.

The complex velocity potential for corner flow with a source of strength m located on the wall at a radius r_0 downstream, is given by

$$\omega = (\alpha/n)z^n - 2m \ln(z^n + r_0^n)$$

and consequently the unperturbed velocity is

$$u_0(z, \bar{z}) = u_{x_0} + iu_{y_0} = \left(\frac{m}{r_0}\right)\bar{z}^{n-1} \left[\frac{2n}{\bar{z}^n + 1} - \chi\right], \tag{20}$$

where $\chi = \alpha r_0^n/m$, and z is replaced by z/r_0 . When (20) is multiplied by its conjugate, non-dimensional groups formed and finally the gradient operator, defined by $(2/r_0)(\partial/\partial\bar{z})$, applied, one has

$$\frac{v'r_0}{m} = \xi z^{n-1} \left[\frac{2n}{z^n + 1} - \chi\right] F = \xi EF, \tag{21}$$

where $\xi = \alpha r r_0^{n-2}$ and

$$F = \bar{z}^{n-2} \left[\frac{2n}{\chi} \frac{n-1-\bar{z}^n}{(\bar{z}^n + 1)^2} + 1 - n\right].$$

Then, by using (20), the particle velocity becomes

$$vr_0/m = \bar{E} - \xi EF, \tag{22}$$

where the bar denotes the conjugate.

The divergence of (21), defined by $2/r_0 \operatorname{Re}(\partial/\partial z)$, is

$$\nabla \cdot \left(\frac{v'r_0}{m}\right) = -\frac{2\chi\xi}{r_0} \operatorname{Re}(F\bar{F}), \tag{23}$$

where Re denotes the real part. The particle density equation, found by substituting (22) and (23) into (9), is then

$$\operatorname{Re}(\bar{E} - \xi EF) \frac{\partial \ln(k/k_0)}{\partial x} + \operatorname{Im}(\bar{E} - \xi EF) \frac{\partial \ln(k/k_0)}{\partial y} = 2\chi\xi \operatorname{Re}(F\bar{F}). \tag{24}$$

The integral surface of this equation is given by the intersection of the two characteristic surfaces formed by the two ordinary differential equations derivable from it by the method of characteristics. To obtain numerical solutions of (24) it is more convenient to introduce a parameter s and to write the two ordinary differential equations as the following three:

$$\left. \begin{aligned} dx/ds &= \operatorname{Re}(\bar{E} - \xi EF), \\ dy/ds &= \operatorname{Im}(\bar{E} - \xi EF), \\ d \ln(k/k_0)/ds &= 2\chi\xi \operatorname{Re}(F\bar{F}). \end{aligned} \right\} \tag{25}$$

The system of equations (25) can, under certain circumstances, be solved reasonably easily by using the Runge–Kutta method. This is done by choosing a barrier to eliminate problems of multivaluedness and restricting the values of n

to allow the use of a standard subprogram for square roots to compute the roots of the complex quantities. It is found, however, that for values of n near unity this model provides a poor representation of corner flow separation. The reason is that a 'flare' projects out from the corner, and the wall streamline at the origin, instead of being of infinite radius as on a free streamline, turns abruptly almost at right angles to the direction of approach. The model seems satisfactory for values of n near $\frac{1}{2}$, and the flow corresponding to $n = \frac{1}{2}$ is chosen for evaluation here.

To compute the delineation curves, the first two of equations (25) are first integrated for $\chi = 1$; the limiting case of $\xi \rightarrow 0$ then yields the fluid separation line. These curves are all shown in figure 2. It is evident that the disappearance of the infinite velocity at the origin reduces considerably the magnitude of the perturbation. The curves representing $\xi = 1$ are of qualitative use only, since this value is somewhat large.

The complete set of equations (25) is then integrated downstream, from an upstream point on the streamline $c = 1.5$, for $\chi = 2n = 1$ and $\chi = 10^4$ and different values of ξ ; the latter value of χ yielding the unseparated flow. The particle streamlines, as shown in figure 4, indicate that, even at short distances from the corner, the perturbation has been reduced to an almost insignificant size by the separation.

How separation will affect convex flows other than that presented here may be qualitatively inferred from the present results. Since the case $n = \frac{1}{2}$ produces the largest perturbation of any convex flow, and in this case the perturbation is considerably reduced due to the separation, it seems reasonable to assume that, for values of n near unity, the separation would virtually negate the effects of the perturbation.

The particle density distributions along some of the streamlines of figures 3 and 4 are shown in figure 5. No attempt is made to present the distributions along the delineation curves because, due to the singularity, the derivatives of k are undefined there.

5. Summary

The assumption of arbitrary initial particle density k_0 leads to a system of equations that seems to have neither a simple analytical, nor a simple numerical, solution, and is not treated here. If one further assumes that k_0 is small, such solutions are available.

Regardless of whether separation is considered, the solution centres around the particle density equation. This first-order partial differential equation can be solved by the method of characteristics, which yields ordinary differential equations that may be solved numerically by the Runge-Kutta method. The characteristic base curves are formed by the particle streamlines, and the integral surface of the density equation is represented by the variation in particle density along these streamlines. In unseparated flows, these ordinary differential equations can be solved analytically for several convex cases but, in general, at least a simple numerical integration is required.

The separation model considered here comprises a corner flow combined with a source just downstream of the corner. The model is satisfactory for small values of n , but requires the Runge–Kutta integration procedure.

Convex-type flows always yield particle-free zones. In the unseparated flows, these zones are delineated by spiral-shaped curves, which emanate from the origin at the upstream side, partially encircle it, and then trail downstream. The size of the zones depends largely on the particle relaxation time τ . In separated flows, the singularity in the fluid velocity at the origin disappears and consequently the particle spirals become very much reduced in size.

Of all convex flows, the case of $n = \frac{1}{2}$ is the most strongly affected by the perturbation. Because of the considerable reduction, in this case, in the size of the perturbation, by the separation, it seems reasonable to infer that the effects of separation would practically negate the perturbation, for values of n near unity, i.e. for small convex angles.

The particle density is found to increase monotonically in the downstream direction on all particle streamlines; it increases rapidly in the neighbourhood of the delineation curves and maximizes on them far downstream. With increasing radius from the corner, the density slowly decreases to k_0 . Particle densities resulting from the computations in the neighbourhood of the delineation lines are of limited value, since the singularity across these lines implies undefined density derivatives.

The author wishes to thank Professors Wuest and Grohne for some useful conversations in the course of this work.

REFERENCES

- INCE, E. L. 1956 *Ordinary Differential Equations* (1st American edn.). New York: Dover.
- MICHAEL, D. H. 1968 The steady motion of a sphere in a dusty gas. *J. Fluid Mech.* **31**, 175–192.
- MILNE-THOMSON, L. M. 1968 *Theoretical Hydrodynamics* (5th edn.). London: Macmillan.
- RANNIE, W. D. 1962 *Progress in Astronautics and Rocketry. Detonation and Two-Phase Flow* (ed. S. S. Penner & F. A. Williams), vol. 6. New York: Academic.